Supplementary Information

Interpreting elemental signatures at palm-leaf manuscript inscriptions through historical and experimental evidence using synchrotron XRF

Laura Gallardo, Mark Busch, Giovanni Ciotti, Patrick Huber

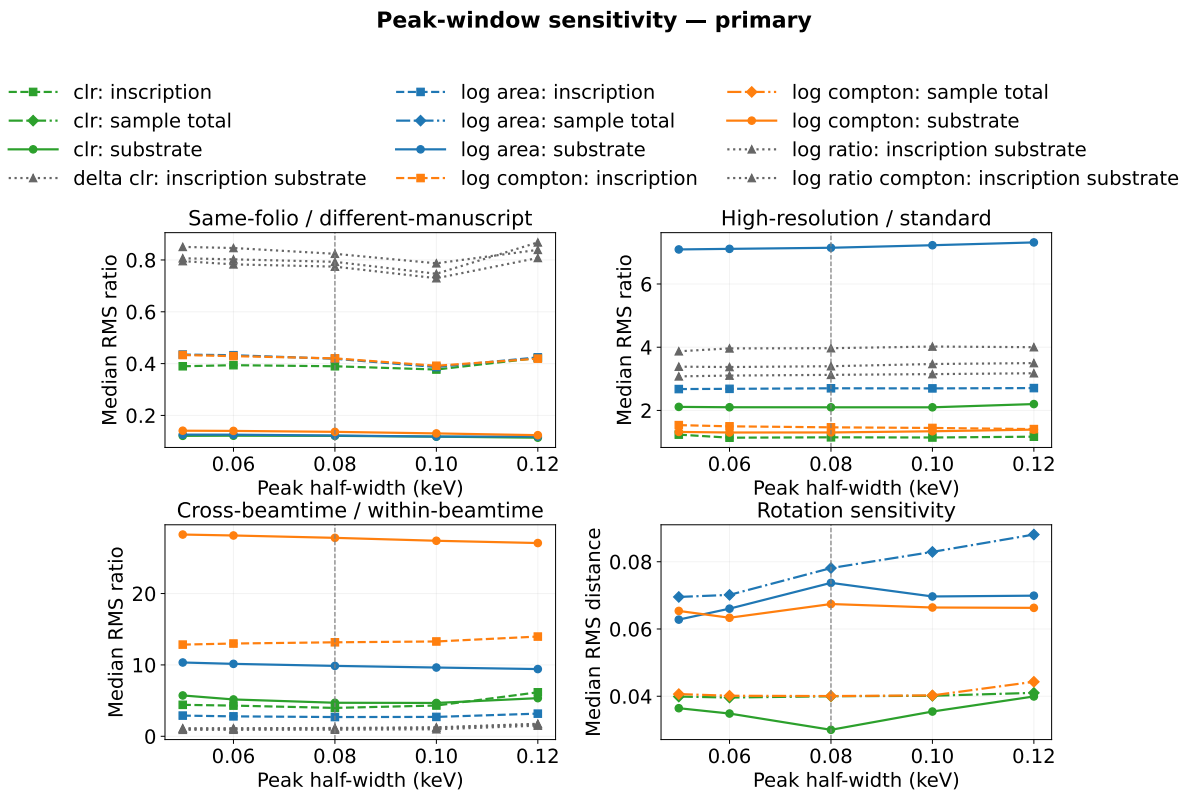
Supplementary Data files

Supplementary Data 1. Table of measurements The separately supplied Excel workbook contains a list of the measurements included in this analysis. In the table it is specified during which beamtime the measurement was taken through the *sample* column. The rows in the table are ordered according to *material type*: first manuscripts (historical objects) and then the mock-up samples, and are ordered in a secondary level alphabetically according to *object*, which is used as object/sample identifier. The *object* column contains the shelf number in the case of the manuscripts (according to the institution in which they are held, the Centre for the Study of Manuscript Cultures CSMC at the University of Hamburg). For the mock-ups, *object* column contains an assigned name. Since they are numbered according to object, all measurements performed on the same object are consecutive in the table. The column *number* numbers the objects in the order they appear in the table. Column *measurement* indicates the measurement name assigned during the beamtimes to every measurement, and *alpha (°)* the angle between the beam and the plane of the sample. Column *folio/fragment* indicates the folio or fragment number in which the measurement was performed, when applicable. Columns *inscription*, *hole*, *colored*, *edge* take values *yes* or *no* indicating whether the scan area contains an inscription, a hole, an inscription with apparent darkening procedure, or a folio edge, respectively. Columns *stylus* amd *writing support* are empty for all manuscripts. In these it is specified which kind of stylus and in which reference writing support each mockup was prepared. Column *notes* contains general observations made during the inspection of elemental maps and object images. Measurements performed at the highest resolution during the first beamtime (sample 0) are labeled with *HR*.

Assessment of analytical robustness and measurement comparability

The robustness of the elemental profiles obtained by direct peak integration was evaluated with respect to peak-integration parameters, measurement geometry, acquisition conditions, and measurement reproducibility. The assessment was performed using locally background-corrected peak areas extracted directly from the XRF spectra. Substrate and inscription profiles were evaluated separately, together with inscription–substrate contrasts.

For each comparison, the difference between two elemental profiles was quantified using the root-mean-square (RMS) distance,



Supplementary Figure 1: Sensitivity of the consistency metrics to the peak-integration half-width. The panels show the ratio between repeated same-folio and different-manuscript distances, the ratio between high-resolution and standard same-folio distances, the cross-beamtime/within-beamtime distance ratio, and the median RMS distance associated with sample rotation. The vertical dashed line indicates the selected half-width of ±0.08 keV.

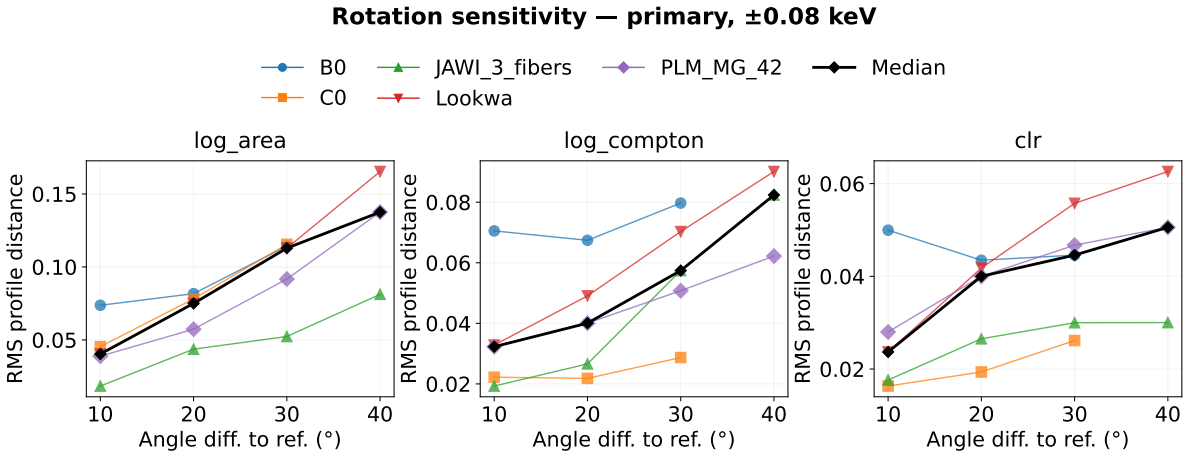
$$d_{\mathrm{RMS}}(x, y) = \sqrt{\frac{1}{E}\sum_{e=1}^{E}(x_e - y_e)^2},$$

where x_e and y_e are the transformed peak areas or elemental contrasts for element e, and E is the number of elements included in the comparison. No feature-wise autoscaling was applied; RMS distances were calculated directly in the units of each representation. When multiple scan pairs represented the same folio or manuscript comparison, their distances were aggregated at the corresponding comparison-unit level before summary statistics were calculated, preventing repeatedly measured objects from receiving disproportionate weight.

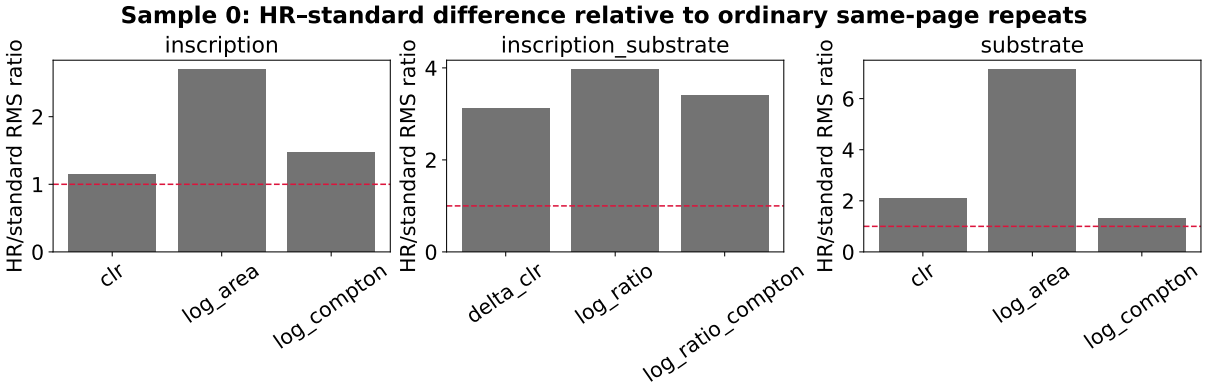
Sensitivity to peak-integration parameters

The influence of the peak-integration window was assessed using half-widths of 0.05, 0.06, 0.08, 0.10, and 0.12 keV around the selected elemental lines. For each window, the resulting profiles were evaluated using within-beamtime repeatability, standard- versus high-resolution acquisition, cross-beamtime comparability, and rotation sensitivity.

The principal consistency metrics changed only moderately over the tested range around the selected value, and no systematic improvement was obtained by increasing the integration width. A half-width of 0.08 keV was therefore retained for the subsequent analyses.



Supplementary Figure 2: Sensitivity of elemental profiles to sample rotation for the different representations. RMS distances are calculated relative to the reference orientation. Individual markers identify the rotation series and the black curve shows the median at each angular difference.



Supplementary Figure 3: Difference between standard- and high-resolution acquisitions relative to ordinary standard-resolution repeats of the same folio. A ratio of 1 (dashed line) corresponds to the median distance between ordinary same-folio repeats; values above 1 indicate larger differences between high- and standard-resolution acquisitions.

Influence of sample rotation and acquisition resolution

The influence of sample orientation was examined using rotation series acquired at different angular positions. Elemental profiles were compared with the corresponding reference orientation. Log-transformed peak areas, Compton-normalised peak areas, and centered log-ratio (CLR) coordinates were evaluated separately.

Rotation produced representation- and sample-dependent changes, but the CLR representation showed comparatively limited sensitivity to orientation. Rotation was therefore considered a contributing source of variability but did not account for the larger differences observed between some manuscript measurements.

Standard- and high-resolution acquisitions were additionally compared using measurements of the same manuscript and folio in sample 0. Their RMS differences were expressed relative to ordinary standard-resolution same-folio repeats.

High- versus standard-resolution differences generally exceeded ordinary same-folio repeatability, with the magnitude depending on the elemental representation and region. High-resolution

Supplementary Table S1: Number of profiles available for conventional 13-element CLR and fixed-reference mCLR. mCLR requires positive areas for the six reference elements but permits non-reference elements to be evaluated individually when detected.

Region	CLR, sample 0	mCLR, sample 0	CLR, sample 3	mCLR, sample 3
Substrate	34	56	0	22
Inscription	23	47	0	17
Inscription–substrate	18	47	0	17

measurements were consequently tracked separately when evaluating cross-beamtime comparisons rather than being treated as directly interchangeable with standard acquisitions.

Within- and cross-beamtime reproducibility

Within each beamtime, standard-resolution measurements were classified as repeated measurements of the same folio, measurements of different folios of the same manuscript, or measurements of different manuscripts. This provided an empirical scale against which acquisition-related variability could be compared with within- and between-manuscript heterogeneity.

Several representations were considered: logarithmic peak areas, Compton-normalised logarithmic peak areas, and CLR coordinates for standalone substrate and inscription profiles; and direct logarithmic inscription–substrate ratios and differences between inscription and substrate CLR coordinates (ΔCLR) for regional contrasts. The combined consistency tests were used to select a relative-composition representation for comparisons among measurements. Direct log ratios were retained for element-specific local enrichment because they retain the magnitude and direction of the regional signal change, whereas CLR-based contrasts were used for comparisons of relative elemental signatures across measurements.

Detailed within-beamtime distributions, pair-level results, and element-by-element cross-beamtime comparisons are provided with the analysis notebook and numerical outputs in the accompanying repository [1].

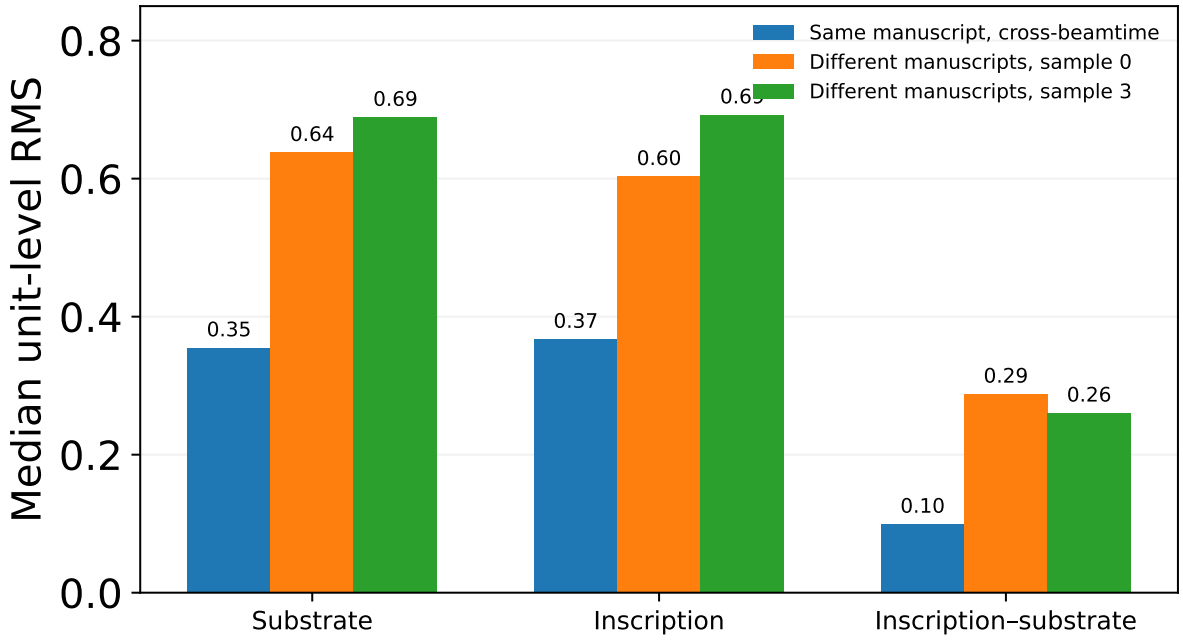
Extension to the fixed-reference mCLR representation

Conventional CLR requires positive integrated areas for every element included in the transformation. Because this condition was not fulfilled uniformly for the complete 13-element set, the analysis of historical manuscripts used a modified CLR (mclr) referenced to the fixed set Al, Ca, Fe, K, Mn and Zn.

The principal consistency analyses described above were performed using this same six-element reference set. For these six elements, mclr is mathematically equivalent to a conventional CLR calculated over the reference set. A separate complete-case comparison was additionally performed between 13-element CLR profiles and six-element-reference mCLR profiles wherever all 13 peak areas were positive. On this restricted subset, the two transformations gave closely comparable distance structures. For example, median substrate RMS distances between different manuscripts were 0.903 for CLR and 0.941 for mCLR, whereas repeated measurements of the same folio gave 0.250 and 0.258, respectively.

The fixed-reference transformation substantially increased data availability. In particular, none of the sample 3 profiles contained positive areas for all 13 elements, whereas mCLR retained 22 substrate and 17 inscription profiles. A direct cross-beamtime comparison between 13-element CLR and mCLR was therefore not possible. Instead, the consistency of the fixed reference itself was evaluated across both beamtimes using the six common reference elements.

Repeated substrate measurements of the same folio showed similar variability in the two beamtimes, with median RMS distances of 0.074 in sample 0 and 0.087 in sample 3. Different-



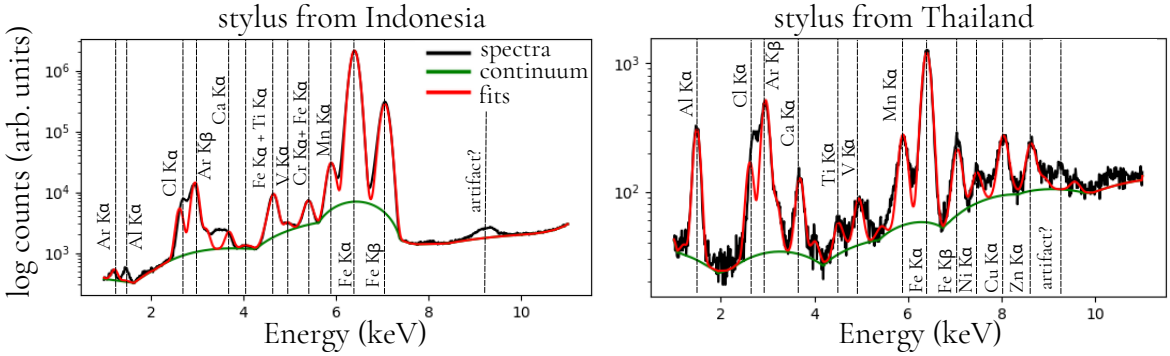
Supplementary Figure 4: Cross-beamtime comparability of fixed-reference elemental profiles. Median RMS distances calculated using the six reference elements (Al, Ca, Fe, K, Mn and Zn) are shown for measurements of the same manuscript acquired in different beamtimes and for measurements of different manuscripts within each beamtime. Substrate and inscription profiles are shown together with inscription–substrate contrasts (ΔmCLR). Multiple scan-level comparisons were first aggregated by independent folio or manuscript comparison unit. Cross-beamtime comparisons comprised nine substrate units and six inscription and therefore inscription–substrate units. Most cross-beamtime units correspond to different or non-identically labelled folios of the same manuscript and therefore assess manuscript-level comparability rather than direct instrumental repeatability.

folio comparisons in sample 3 were more variable and were based on only three independent manuscript–folio comparison units; these measurements were retained because the limited sample does not provide sufficient evidence to classify them as analytical outliers.

At manuscript level, the median cross-beamtime distance was smaller than the median distance between different manuscripts within either beamtime for substrate profiles, inscription profiles, and inscription–substrate contrasts. The corresponding cross-beamtime medians were 0.355, 0.367 and 0.099, respectively, compared with between-manuscript medians of 0.638, 0.603 and 0.287 in sample 0 and 0.689, 0.692 and 0.260 in sample 3.

Together, these checks support the use of the fixed-reference representation for comparisons across the combined manuscript dataset while retaining the observed folio-level variability as part of the material variation rather than removing individual measurements post hoc. Complete pair-level distances, diagnostic figures, and numerical summaries are provided in the accompanying repository.

XRF measurement of Indonesian and Thai styluses



Supplementary Figure 5: XRF spectra of two styluses used experimentally to inscribe palm-leaf writing supports, measured with Crono, with a exposure time of 120 s. Black curves correspond to the measured spectra, green curves to the fitted continuum, and red curves to the fitted elemental contributions, both were calculated in pyMCA [2]. Peak assignments are indicated.

References

1. Gallardo, L., Busch, M. & Huber, P. *Analysis of elemental signatures at palm-leaf manuscripts inscriptions* (TORE, 2026).
2. Solé, V. A., Papillon, E., Cotte, M., Walter, P. & Susini, J. A multiplatform code for the analysis of energy-dispersive X-ray fluorescence spectra. *Spectrochimica Acta Part B: Atomic Spectroscopy* **62,** 63–68 (2007).